

## Viscosity of CHF<sub>3</sub> in the Critical Region

C. Yokoyama<sup>1,2</sup> and M. Takahashi<sup>1</sup>

*Received May 1, 1997*

---

The gaseous viscosity of trifluoromethane (CHF<sub>3</sub>) was measured in the critical region. The experimental temperature range was between 299.150 and 303.150 K and the pressure range was up to 5.66 MPa. The measurements were obtained with an oscillating-disk viscometer, combined with local determination of the density at the position of the oscillating disk, and they have an estimated accuracy of 0.6% for the viscosity and 0.5% for the gas density. The viscosity of CHF<sub>3</sub> exhibits an anomalous increase near the critical point. The anomalous increase in viscosity was analyzed with the viscosity equation proposed by Basu and Sengers.

---

**KEY WORDS:** critical anomaly; mode-coupling theory; trifluoromethane; viscosity.

### 1. INTRODUCTION

The viscosity of fluids in the critical region exhibits an anomalous increase. In a previous study, we reported the viscosity of carbon dioxide, ethane, and nitrous oxide in the critical region [1–3]. As part of a continuing study of the viscosity of dense fluid systems, measurements of the viscosity of trifluoromethane (CHF<sub>3</sub>), made between 299.150 and 303.150 K at pressures up to 5.66 MPa, are reported.

The viscosity of gaseous CHF<sub>3</sub> at normal pressure has been measured by Coughlin [4], McCullum [5], Kamien and Witzell [6], Tsui [7], and Wilbers [8]. These data have been compiled by Witzell and Johnson [9]. Altunin et al. [10] reported a table of viscosity at high pressures compiled from experimental data of Ivanchenko [11], Raskazov et al. [12–14], and Sagaedakova [15]. However, the viscosity of CHF<sub>3</sub> in the critical region has not yet been measured.

---

<sup>1</sup> Institute for Chemical Reaction Science, Tohoku University, 2-1-1 Katahira, Aoba-ku, Sendai 980-77, Japan.

<sup>2</sup> To whom correspondence should be addressed.

## 2. EXPERIMENTAL PROCEDURE

The viscosity was measured with an oscillating-disk viscometer and the density was measured with a high-pressure gas pipette. The experimental apparatus and procedure are principally the same as those described in previous papers [1-3, 16-19]. Therefore, the details of the apparatus and procedure are not presented in this paper.

The results of the measurements were evaluated with the aid of Newell's theory [20] in a manner similar to that used by Iwasaki and Kestin [21]. The viscosity is given by the following equation:

$$\eta = 2\pi\rho b^2/\beta^2 T_0 \quad (1)$$

where  $\eta$  represents the viscosity,  $\rho$  the density,  $b$  the harmonic mean of the distances between the oscillating disk and the upper and lower fixed disks,  $T_0$  the period of oscillation *in vacuo*, and  $\beta$  the ratio of  $b$  to the boundary layer thickness. On the other hand,  $\beta^2$  was determined from the measured values of the logarithmic decrement  $\Delta$  and period of oscillation  $T$  from the cubic equation,

$$C_N = \left[ \frac{2I}{\pi\rho b R^4} \left( \frac{\Delta}{\tau} - \Delta_0 \right) + a \frac{\Delta}{\tau} \right] \beta^2 + f \frac{\Delta^2 - 1}{\tau^2} \beta^4 + h \frac{\Delta(\Delta^2 - 1)}{\tau^3} \beta^6 \quad (2)$$

in which all terms of order  $\Delta^3$  or higher have been neglected with respect to unity. Here  $\Delta$  denotes the decrement of damping evaluated over 10 consecutive cycles. Further,  $I$  denotes the moment of inertia of the suspension,  $R$  is the radius of the oscillating disk, and  $\tau$  denotes the ratio

$$\tau = T/T_0 \quad (3)$$

of the actual period of oscillation to that *in vacuo*. The factors  $a$ ,  $f$ , and  $h$  depend on the separations of disks only and are defined as  $a = 2/3$ ,  $f = 1/45$ , and  $h = 8/945$ , if  $b_1 = b_2$ . It was confirmed that the present measurements satisfactorily fulfill the condition for which Eqs. (1) and (2) will yield the required accuracy of 0.1%.

At the experimental temperatures and densities, the edge-correction factor  $C_N$  was obtained by using nitrogen as a standard. The viscosity data for nitrogen were taken from the compilation of Stephan et al. [22] and the density data were obtained from the equation of state proposed by Jacobsen and Stewart [23].

The pressure of the sample was measured with a mercury U-tube detector and a deadweight gauge. The accuracy of the pressure measurements is estimated to be 10 kPa. The temperature of the thermostat was

measured with a quartz thermometer calibrated against a Leed-Northrup platinum resistance thermometer and was kept constant to about  $\pm 0.003$  K over the period of the measurements. The temperature of the viscometer was kept to within 0.001 K. The accuracy of the temperature measurements is estimated to be  $\pm 0.003$  K. The local density was measured with a high-pressure gas pipette and low-pressure gas expansion system. The pipette was equipped with two valves, one of which leads to the low-pressure system and the other to the viscometer, and set horizontally on its supports so that its inner space was kept at the same level as that of the oscillating disk in the viscometer. This configuration of oscillating disk and gas pipette was adopted from a density distribution due to gravity force near the critical point. The details of the gas pipette and density determination were described by Iwasaki and Takahashi [2]. It should be noted that the accuracy of the density measurements is determined from the *PVT* measurements in the low-pressure system. The accuracy of the density measurements is estimated to be 0.4%. The accuracy of the present viscosity measurements is at worst  $\pm 0.6\%$  considering the uncertainties in the determination of the logarithmic decrement, the period of oscillation, the density of the gas, and other sources of error.

The CHF<sub>3</sub> was obtained from Asahi-Glass Co. Ltd., with a stated purity of better than 99.5 mol%, and was used in this experiment without further purification.

### 3. RESULTS AND DISCUSSION

The experimental results are presented in Table I. Figure 1 shows a comparison of the present data for the viscosity at normal pressure with literature data of Coughlin [4], Kamien and Witzell [6], and Wilbers [8] and compiled values of Altunin et al. [10]. It can be seen that the present results agree well with the compiled values of Altunin et al. [10]. The deviations of the present data for the viscosity at 303.15 K and, under high pressures, from those compiled by Altunin et al. [10] are shown in Fig. 2. In the low-density region, less than  $200 \text{ kg} \cdot \text{m}^{-3}$ , the present viscosity data are lower than the literature data, while in the high-density region the present data are higher. The average absolute and maximum deviations were 3.0 and 5.9%, respectively. Figure 3 shows a plot of the viscosity versus the pressure. The viscosity increases rapidly near the critical point. In Figs. 4 and 5, the viscosity is plotted against the density for the same temperatures. Figure 5 represents the critical region in more detail. It can be seen from Figs. 4 and 5 that the viscosity exhibits an anomalous increase near the critical point. The present results may be the first to reveal the critical anomaly of the viscosity of CHF<sub>3</sub>.

Table I. Viscosity of CHF<sub>3</sub>

$P$ (MPa)	$\rho$ (kg · m <sup>-3</sup> )	$\eta$ ( $\mu$ Pa · s)	$P$ (MPa)	$\rho$ (kg · m <sup>-3</sup> )	$\eta$ ( $\mu$ Pa · s)
$T = 299.150$ K			4.8227	597.91	39.445
0.1014	2.877	14.782	4.8270	613.34	40.133
0.3888	11.277	14.807	4.8292	622.83	40.757
0.6929	20.601	14.825	4.8361	634.89	41.484
1.0880	33.500	14.928	4.8414	643.59	42.312
1.5066	48.296	15.018	4.8538	657.04	43.150
1.9656	65.964	15.207	4.8658	667.40	43.962
2.3773	83.695	15.429	4.8791	677.70	44.904
2.7465	101.83	15.716	4.9016	689.36	45.704
3.0721	119.84	16.028	4.9232	698.55	46.717
3.3564	137.65	16.389	4.9531	708.86	47.581
3.6032	155.41	16.804	4.9831	718.31	48.366
3.8191	172.82	17.226	5.0202	728.18	49.388
4.0056	190.70	17.678	5.0666	737.93	50.321
4.1653	208.70	18.203	5.1201	747.96	51.330
4.3001	226.41	18.739	5.1948	759.97	52.435
4.4133	244.38	19.300	5.2542	772.72	53.612
4.5082	262.45	19.869	5.3537	784.09	54.782
4.5765	278.62	20.496	5.4678	792.66	55.437
4.6362	295.66	21.137	$T = 299.350$ K		
4.6831	311.85	21.843	0.1017	2.882	14.803
4.7250	329.57	22.546	0.4058	11.778	14.799
4.7476	344.20	23.249	0.6872	20.407	14.828
4.7663	358.52	23.901	1.0636	32.647	14.875
4.7813	371.69	24.592	1.5045	48.169	15.018
4.7913	384.33	25.279	2.2127	76.407	15.319
4.7995	397.38	26.117	2.5922	93.788	15.581
4.8063	412.24	27.078	2.9239	111.06	15.849
4.8106	427.04	28.100	3.2131	128.10	16.167
4.8127	437.54	28.988	3.4667	144.77	16.483
4.8151	450.10	30.542	3.6845	161.16	16.924
4.8154	461.87	31.215	3.8717	177.04	17.281
4.8164	468.09	32.772	4.0378	193.32	17.747
4.8171	483.34	35.599	4.1794	209.08	18.181
4.8177	496.88	35.807	4.3003	224.87	18.651
4.8178	528.07	37.432	4.4036	240.53	19.156
4.8180	541.90	37.148	4.4934	256.66	19.694
4.8182	547.60	37.110	4.5688	273.35	20.282
4.8184	560.60	37.947	4.6286	288.06	20.859
4.8192	570.33	37.942	4.6792	304.10	21.468
4.8195	568.86	38.139	4.7190	319.54	22.125
4.8196	577.16	37.964	4.7488	333.49	22.715
4.8212	584.95	38.855			

Table I. (Continued)

$P$ (MPa)	$\rho$ (kg · m <sup>-3</sup> )	$\eta$ ( $\mu$ Pa · s)	$P$ (MPa)	$\rho$ (kg · m <sup>-3</sup> )	$\eta$ ( $\mu$ Pa · s)
4.7731	347.92	23.393	1.0782	33.092	14.894
4.7924	362.57	24.106	1.5591	50.115	15.032
4.8075	377.77	24.884	1.9585	65.430	15.196
4.8182	395.15	25.686	2.3211	80.919	15.395
4.8256	404.71	26.452	2.6394	95.951	15.602
4.8314	420.68	27.707	2.9393	111.60	15.898
4.8359	436.74	28.606	3.1946	126.56	16.166
4.8372	446.40	29.787	3.4351	141.39	16.482
4.8395	460.84	31.551	3.6498	157.55	16.853
4.8418	484.28	33.181	3.8377	173.12	17.206
4.8426	495.98	34.488	4.0026	188.55	17.617
4.8427	499.61	35.097	4.1483	204.00	18.044
4.8438	517.69	35.926	4.2667	218.40	18.464
4.8449	535.86	36.532	4.3682	232.57	18.916
4.8451	545.48	36.708	4.4660	248.62	19.439
4.8454	546.68	37.057	4.5482	263.91	19.973
4.8456	555.23	37.201	4.6164	279.77	20.555
4.8470	569.40	37.950	4.6711	294.18	21.089
4.8492	583.50	38.424	4.7159	309.38	21.755
4.8500	583.74	38.691	4.7542	324.90	22.364
4.8522	593.71	39.095	4.7843	340.15	23.062
4.8548	605.56	39.869	4.8091	355.47	23.738
4.8599	620.43	40.704	4.8253	369.89	24.407
4.8671	634.70	41.536	4.8393	384.56	25.272
4.8761	646.53	42.338	4.8507	398.54	26.039
4.8853	654.67	43.007	4.8570	411.68	26.969
4.9004	667.75	43.996	4.8633	426.08	27.907
4.9134	676.95	44.776	4.8674	438.39	29.063
4.9308	685.36	45.563	4.8711	452.91	30.144
4.9523	695.16	46.327	4.8747	471.14	31.296
4.9782	705.16	47.177	4.8764	478.22	32.336
5.0105	714.71	48.028	4.8774	490.18	33.382
5.0503	724.51	48.909	4.8790	504.36	34.397
5.0916	733.99	49.893	4.8812	526.94	35.182
5.1428	744.50	50.879	4.8830	539.03	36.015
5.2076	755.18	51.908	4.8851	550.55	36.816
5.2823	765.74	52.975	4.8873	559.87	37.392
5.3691	776.71	54.026	4.8889	575.30	38.114
			4.8914	585.70	38.665
			4.8953	597.74	39.191
			4.9000	611.44	40.031
			4.9081	626.24	41.018
			4.9182	640.74	42.024
			4.9392	655.90	43.216
	$T = 299.650$ K				
0.1018	2.8820	14.800			
0.3912	11.326	14.815			
0.6933	20.574	14.818			

Table I. (Continued)

$P$ (MPa)	$\rho$ ( $\text{kg} \cdot \text{m}^{-3}$ )	$\eta$ ( $\mu\text{Pa} \cdot \text{s}$ )	$P$ (MPa)	$\rho$ ( $\text{kg} \cdot \text{m}^{-3}$ )	$\eta$ ( $\mu\text{Pa} \cdot \text{s}$ )
4.9613	672.31	44.533	4.9977	522.10	33.483
4.9920	688.08	45.689	5.0003	534.94	34.405
5.0273	699.74	46.903	5.0062	550.98	35.383
5.0636	712.36	47.992	5.0128	566.78	36.272
5.1058	725.20	48.915	5.0161	576.01	36.860
5.1517	733.80	49.932	5.0216	586.31	37.725
5.2074	745.80	50.861	5.0288	598.75	38.297
	$T = 300.65 \text{ K}$		5.0347	607.21	39.035
			5.0424	616.86	39.718
0.1016	2.8670	14.850	5.0496	624.21	40.311
0.1018	2.8740	14.843	5.0583	634.24	40.893
0.5036	14.657	14.864	5.0685	642.37	41.638
0.9136	27.513	14.890	5.0780	651.49	42.281
1.4381	45.437	15.005	5.0933	661.05	43.009
1.9003	62.833	15.236	5.1117	670.53	43.749
2.3129	80.168	15.408	5.1280	678.31	44.522
2.6861	97.478	15.700	5.1526	688.55	45.399
3.0190	115.56	15.952	5.1781	698.63	46.250
3.3079	132.14	16.344	5.2125	705.87	46.918
3.5718	149.81	16.717	5.2478	715.41	47.831
3.7965	167.05	17.108	5.2902	726.27	48.832
3.9926	184.17	17.525	5.3493	736.72	49.806
4.1632	200.69	18.029	5.4051	745.62	50.638
4.3094	218.54	18.465	5.4742	756.09	51.774
4.4326	235.34	19.034	5.5559	767.36	52.878
4.5405	252.86	19.593			
4.6291	269.63	20.129		$T = 303.150 \text{ K}$	
4.6971	285.41	20.749			
4.7557	301.38	21.390	0.1015	2.8410	14.973
4.8039	317.28	22.051	0.4356	12.492	14.995
4.8417	336.12	22.644	0.8253	24.356	15.030
4.8746	347.21	23.390	1.2839	39.378	15.137
4.8986	362.55	24.082	1.7064	54.560	15.267
4.9213	379.17	24.831	2.0957	69.757	15.434
4.9257	393.99	25.462	2.4577	85.154	15.641
4.9479	407.45	26.332	2.7852	100.60	15.880
4.9586	420.98	27.194	3.0750	115.70	16.132
4.9687	434.69	27.958	3.3424	130.83	16.469
4.9740	451.64	28.895	3.5735	145.21	16.776
4.9797	465.39	29.712	3.7899	160.45	17.144
4.9829	473.01	30.295	3.9825	175.94	17.574
4.9879	488.27	31.211	4.1539	190.99	17.903
4.9924	504.82	32.226	4.3006	205.75	18.340
4.9966	521.86	33.025	4.4368	220.61	18.722

Table I. (Continued)

$P$ (MPa)	$\rho$ ( $\text{kg} \cdot \text{m}^{-3}$ )	$\eta$ ( $\mu\text{Pa} \cdot \text{s}$ )	$P$ (MPa)	$\rho$ ( $\text{kg} \cdot \text{m}^{-3}$ )	$\eta$ ( $\mu\text{Pa} \cdot \text{s}$ )
4.5554	235.78	19.236	5.2994	526.79	33.295
4.6579	250.68	19.685	5.3048	530.40	33.845
4.7483	265.66	20.229	5.3116	539.12	34.267
4.8290	280.51	20.759	5.3195	547.60	34.798
4.8958	295.23	21.352	5.3260	555.86	35.308
4.9509	309.11	21.900	5.3357	561.98	35.777
4.9991	322.76	22.418	5.3430	570.42	36.322
5.0408	336.67	22.987	5.3512	578.44	36.854
5.0800	351.38	23.563	5.3618	589.46	37.468
5.1126	365.80	24.288	5.3733	595.57	37.976
5.1400	380.21	24.989	5.3831	605.03	38.641
5.1633	394.11	25.728	5.3971	611.28	39.156
5.1829	407.24	26.391	5.4112	620.28	39.853
5.2012	420.40	27.069	5.4265	629.15	40.554
5.2162	433.71	27.771	5.4447	637.81	41.260
5.2303	446.89	28.542	5.4647	646.80	42.002
5.2432	458.42	29.177	5.4866	656.16	42.756
5.2536	472.10	30.005	5.5115	665.43	43.405
5.2658	482.32	30.714	5.5404	674.68	44.189
5.2746	495.70	31.480	5.5717	683.45	44.999
5.2841	507.68	32.111	5.6114	692.38	45.875
5.2916	518.26	32.770	5.6518	703.70	46.674

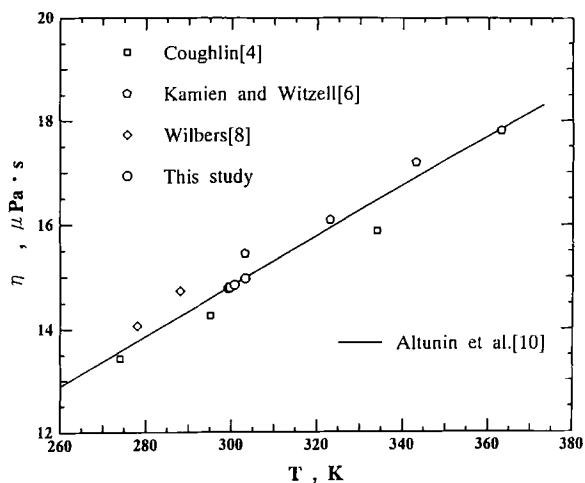


Fig. 1. Viscosity of  $\text{CHF}_3$  at normal pressure.

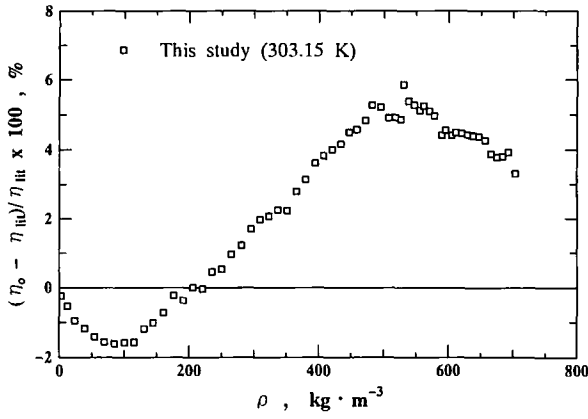


Fig. 2. Deviations of the present viscosity values from those compiled by Altunin et al. [10].

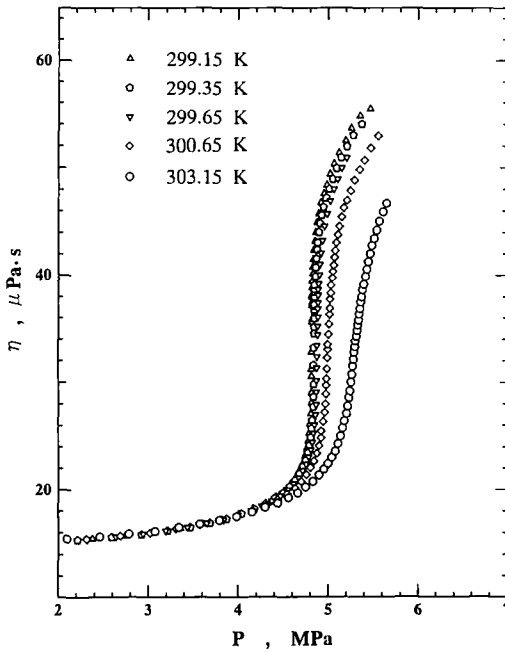


Fig. 3. Viscosity of CHF<sub>3</sub> as a function of pressure.



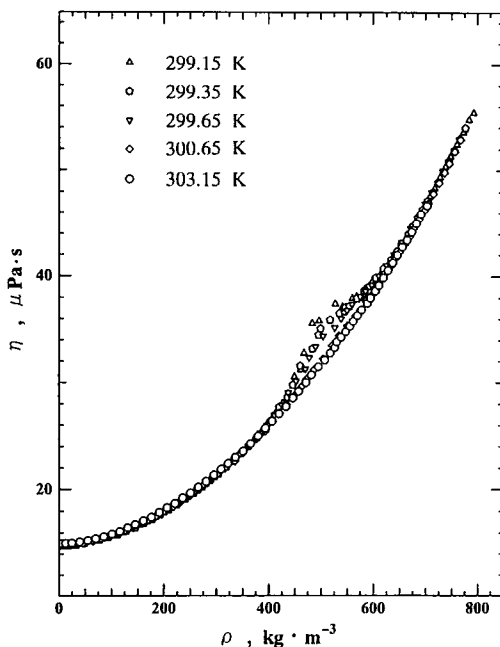


Fig. 4. Viscosity of  $\text{CHF}_3$  as a function of density.

To represent the anomalous behavior of the viscosity in the critical region, it is necessary to know the behavior of a background viscosity [24, 25]. As suggested by Sengers [24], the experimental viscosity  $\eta(\rho, T)$  can be separated into an anomalous part  $\Delta\eta(\rho, T)$  and a background viscosity  $\bar{\eta}(\rho, T)$ , i.e.,

$$\eta(\rho, T) = \bar{\eta}(\rho, T) + \Delta\eta(\rho, T) \quad (4)$$

The background viscosity is obtained empirically by extrapolating the behavior of the viscosity outside the critical region, and it may be written

$$\bar{\eta}(\rho, T) = \eta_0(T) + \eta_c(\rho, T) \quad (5)$$

where  $\eta_0(T)$  is the viscosity in the limit of low densities and  $\eta_c(\rho, T)$  is the excess viscosity. In this study  $\eta_0(T)$  was assumed to be the viscosity at atmospheric pressure. The excess viscosity is defined as follows:

$$\eta_c(\rho, T) = \bar{\eta}(\rho, T) - \eta_0(T) \quad (6)$$

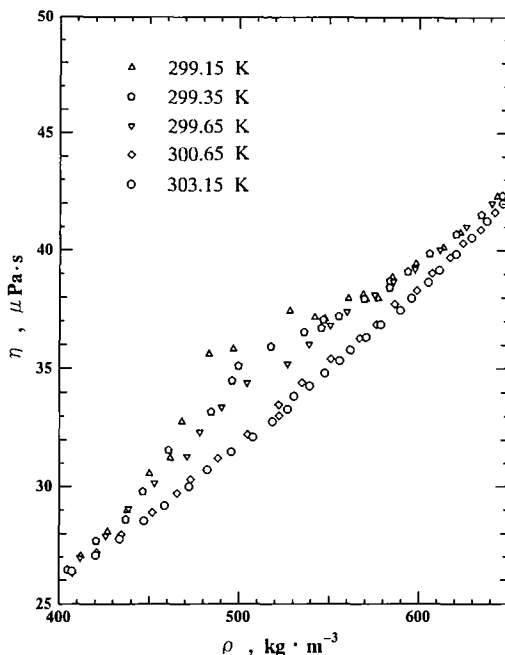


Fig. 5. Viscosity of  $\text{CHF}_3$  in the critical region as a function of density.

In this study the excess viscosity was represented by a simple polynomial in the density:

$$\begin{aligned} \eta_c(\rho, T) &= \bar{\eta}(\rho, T) - \eta_0(T) \\ &= a_1 \rho_c + a_2 \rho_c^2 + a_3 \rho_c^3 + a_4 \rho_c^4 + a_5 \rho_c^5 \end{aligned} \quad (7)$$

where  $\eta$  is in  $\mu\text{Pa}\cdot\text{s}$ ,  $a_i$  are constants, and  $\rho_c$  is an excess density in  $\text{kg}\cdot\text{m}^{-3}$  defined as

$$\rho_c = \rho - \rho_0 \quad (8)$$

where  $\rho_0$  is the density at atmospheric pressure. The values of  $a_i$  at each temperature were determined by fitting the viscosity data outside the critical region, and they are listed in Table II. As can be seen, the values of  $a_i$  vary with temperature.

Since  $\eta_c(\rho, T)$  is established, the background viscosity  $\bar{\eta}(\rho, T)$  can be obtained from Eq. (6). The anomalous viscosity  $\Delta\eta$  can then be obtained

**Table II.** Constants  $a_i$  in Eq. (2)

Temp. [K]	$a_1 \times 10^3$	$a_2 \times 10^5$	$a_3 \times 10^8$	$a_4 \times 10^{10}$	$a_5 \times 10^{14}$
299.15	1.75833	8.43434	-8.01644	1.02700	-4.42404
299.35	1.36738	8.39705	-7.00048	7.70209	-2.62137
299.65	0.858618	9.62092	-14.0463	2.28933	-13.1852
300.65	0.558598	9.78365	-13.5364	1.78096	-7.64937
303.15	1.12993	9.42239	-12.6790	1.87191	-10.0279

from the experimental viscosity and the background viscosity in accordance with Eq. (5). The empirical values thus obtained for  $\Delta\eta$  are shown in Fig. 6. As can be seen,  $\Delta\eta$  exhibits a maximum near the critical density.

Close to the critical point, a simplified theoretical treatment based on the mode-coupling theory yields the following power law [26, 27]:

$$\eta/\bar{\eta} = (q\xi)^\phi \tag{9}$$

where  $q$  is a constant,  $\xi$  is the correlation length, and  $\phi$  is a universal exponent. The original estimate for the value of  $\phi$  from the mode-coupling

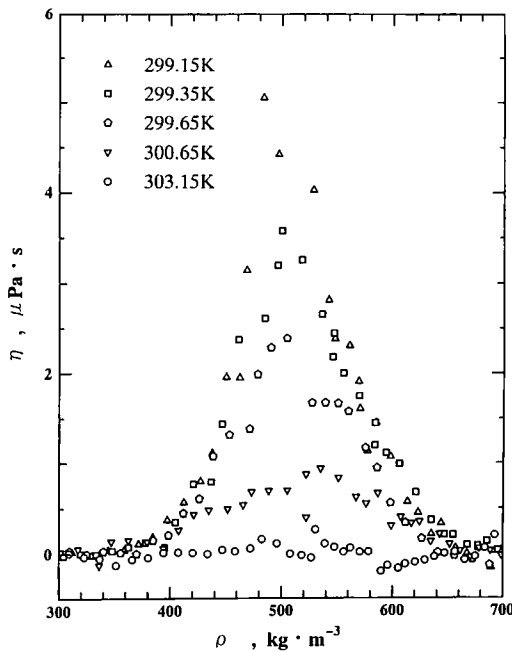


**Fig. 6.** Anomalous viscosity  $\Delta\eta$  of  $\text{CHF}_3$ .

theory is  $8/15\pi^2 = 0.054$ . Recently, it has been shown to be inconsistent with most experimental data for the critical enhancement of the viscosity and should be replaced by a value closer to 0.065 [28–32]. In this study, therefore, we used the value of 0.065 for  $\phi$ . Sengers et al. [24, 26, 27] have suggested that Eq. (9) can be rewritten in terms of the symmetrized isothermal compressibility as follows:

$$\begin{aligned} \eta/\bar{\eta} &= (\chi_{\dagger}^*/\chi_0^*)^{\nu\phi/\gamma} & \text{for } \chi_{\dagger}^* > \chi_0^* \\ \eta/\bar{\eta} &= 1 & \text{for } \chi_{\dagger}^* < \chi_0^* \end{aligned} \tag{10}$$

where  $\chi_{\dagger}^*$  is a reduced symmetrized compressibility,  $\chi_0^* = \Gamma/(q\xi_0)^{\gamma/\nu}$ ,  $\gamma$  and  $\nu$  are critical exponents,  $\Gamma$  is the critical amplitude of  $\chi_{\dagger}^*$ , and  $\xi_0$  is the critical amplitude of  $\xi$ . Equations (9) and (10) are useful for the correlation of viscosity data in the critical region.

According to the mathematical relationships derived by Basu and Sengers [26], the  $\chi_{\dagger}^*$ ,  $\xi_0$ , and  $\zeta$  were calculated with the use of the linear model scaled equation of state. For  $\text{CHF}_3$ , the scaled equation of state was proposed by Aizpiri et al. [33] and Ohgaki et al. [34]. Aizpiri et al. [33]

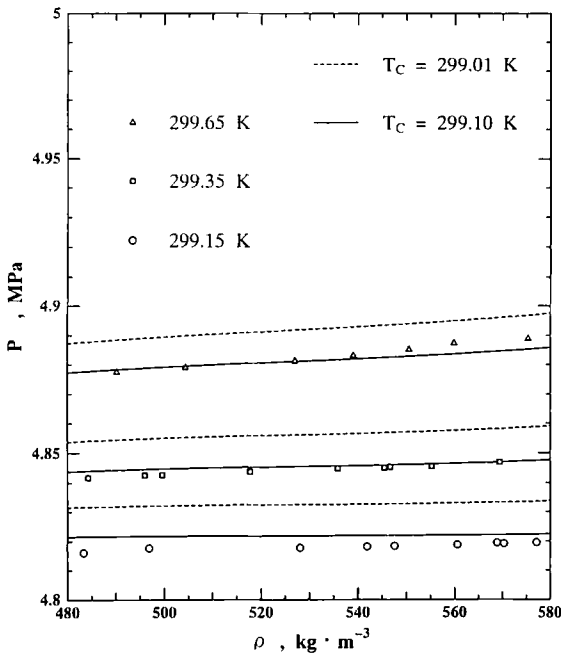


Fig. 7.  $P\rho T$  relationships of  $\text{CHF}_3$  in the critical region.

developed an equation of state based on the critical constants measured by Hori et al. [35]. The critical temperature determined by Ohgaki et al. is about 0.15 K higher than the lowest temperature of our measurements. The calculated values with the scaled equation of state of Aizpiri et al. with the critical-point data,  $T_C$ ,  $\rho_C$ , and  $P_C$ , of Hori et al. and the present data for the  $P\rho T$  relationships in the critical region were compared in Fig. 7. The dashed lines represent the calculated value, which show the systematic deviation from the present data. Therefore the critical temperature value was determined from fitting the calculated pressure to the experimental pressure. In Fig. 7, the  $P\rho$  isotherms calculated with the Aizpiri equation with an optimized  $T_C$  of 299.10 K are shown as solid lines. It can be seen that the present data for the  $P\rho T$  relationships are consistent with the scaled equation of Aizpiri et al. Based on this agreement for the  $P\rho T$  relationship, we decided to use the values of the critical parameters,  $T_C = 299.10$  K, determined in this study,  $\rho_C$  and  $P_C$  determined by Hori et al. [35], and the scaled equation of state of Aizpiri et al. [33] in the following analysis of the critical anomaly.

The values of  $\phi$  and  $q$  can be determined from the double-logarithmic plot of the viscosity ratio  $\eta/\bar{\eta}$  and  $\xi$  as suggested by Basu and Sengers [26]. Figure 8 shows a double-natural logarithmic plot. As suggested by Basu and Sengers [26], it can be seen that at high values of  $\xi$  the data follow a straight line, whose slope yields the effective exponent  $\phi$  and whose intercept on the  $\xi$  axis yields  $q^{-1}$ . However, the values of  $\phi$  and  $q^{-1}$  could not

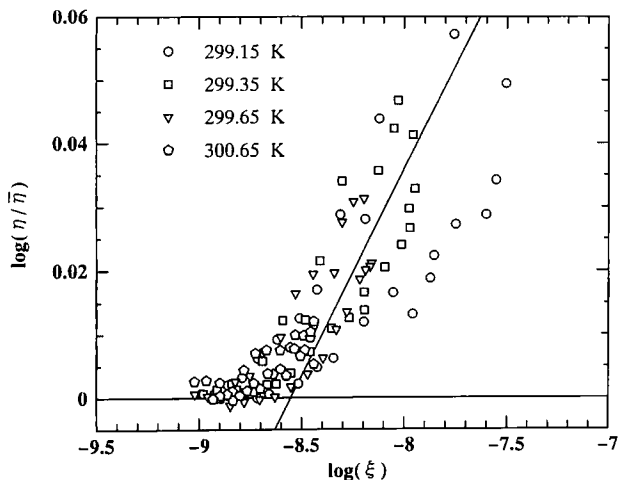


Fig. 8. A double-natural logarithmic plot of the viscosity ratio as a function of the correlation length.

be determined unconditionally with a least-squares fitting of the double-logarithmic plot, in part because of the scatter of the data and of the low magnitude of the critical anomaly of  $\text{CHF}_3$ , compared with the case of  $\text{N}_2$ . Therefore, in this study, the value of  $\phi$  was fixed to the universal value, 0.065, and the value of  $q^{-1}$  was obtained from the data at three isotherms, 299.15, 399.35, and 299.65 K, and in the density range of 461–598  $\text{kg} \cdot \text{m}^{-3}$  (299.15 K), 484–584  $\text{kg} \cdot \text{m}^{-3}$  (299.35 K), and 490–560  $\text{kg} \cdot \text{m}^{-3}$  (299.65 K). The value obtained was  $q^{-1} = 28 \times 10^{-10}$  m.

Table III shows the critical parameters used in this study. According to Eq. (8), the viscosity can be calculated with the results of  $q$ ,  $\phi$ , and the compressibility. A comparison between the calculated results and the experimental data at 299.150 and 303.150 K is shown in Fig. 9. The deviations of the experimental viscosity values from those calculated with Eq. (4) are shown in Fig. 10.

In order to apply the crossover equation proposed by Olchowy and Sengers [36, 37] to the present results, we need a scaled fundamental equation for the thermodynamic properties, e.g., density and isothermal and isobaric heat capacities, of  $\text{CHF}_3$  in the critical region. However, surprisingly few studies have ever tried to derive a scaled equation for  $\text{CHF}_3$ . While Aizpiri et al. [33] and Ohgaki et al. [34] proposed a scaled equation of state for  $\text{CHF}_3$  based on a linear model, they used only the  $P\rho T$  data to determine the parameters of the scaled equation. It would be necessary to refine the scaled equation using data on the specific heat of  $\text{CHF}_3$ . Additional experimental information not only for the viscosity but also for other thermophysical properties, including the thermal conductivity, of  $\text{CHF}_3$  in the critical region are required to analyze the critical viscosity anomaly of  $\text{CHF}_3$  with the theory of dynamic critical phenomena.

Table III. Critical-Region Parameters for  $\text{CHF}_3$

Critical parameters
$T_c = 299.1$ K
$P_c = 4.816 \times 10^6$ Pa
$\rho_c = 529$ $\text{kg} \cdot \text{m}^{-3}$
Critical exponents
$\beta = 0.355$
$\gamma = 1.190$
$\nu = 0.633$
Correlation length scale factor
$\xi_0 = 1.3 \times 10^{-10}$ m

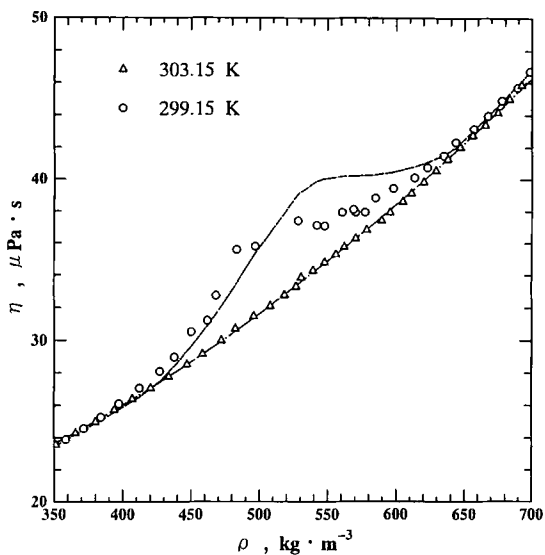


Fig. 9. Comparison between the calculated values and the experimental viscosity at 299.150 and 303.150 K.

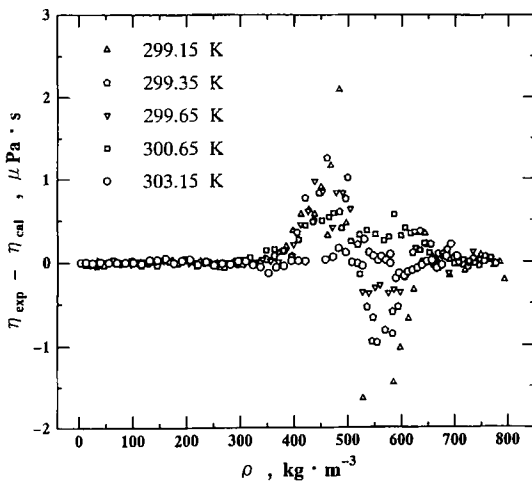


Fig. 10. Deviations of the experimental viscosity values of  $\text{CHF}_3$  from those calculated with Eq. (4).

#### 4. CONCLUSION

We made measurements of the gas viscosity of  $\text{CHF}_3$  in the critical region with the use of an oscillating-disk viscometer. A critical anomaly could be observed at the viscosity isotherms at 299.150, 299.350, and 299.650 K. The viscosity equation derived from the mode-coupling theory was applied to fit the experimental data. It was found that our data obeyed the viscosity equation from the mode-coupling theory.

#### ACKNOWLEDGMENT

This work was funded by Grant-in-Aid for Scientific Research 04238102 from the Ministry of Education, Science, Sport and Culture of Japan, which is gratefully acknowledged.

#### REFERENCES

1. H. Iwasaki and M. Takahashi, *J. Chem. Phys.* **74**:1930 (1981).
2. H. Iwasaki and M. Takahashi, in *Proceedings of the 4th International Conference on High Pressure*, Kyoto (1974), p. 523.
3. C. Yokoyama, M. Takahashi, and S. Takahashi, *Int. J. Thermophys.* **15**:603 (1994).
4. J. Coughlin, M.S. thesis (Purdue University, West Lafayette, IN, 1953).
5. R. G. McCullum, M.S. thesis (Purdue University, West Lafayette, IN, 1958).
6. C. Kamien and O. Witzell, *ASHRAE Trans.* **65**:663 (1959).
7. C. Y. Tsui, M.S. thesis (Purdue University, West Lafayette, IN, 1959).
8. O. J. Wilbers, M.S. thesis (Purdue University, West Lafayette, IN, 1961).
9. O. Witzell and J. Johnson, *ASHRAE Trans.* **71**:30 (1965).
10. V. V. Altunin, V. Z. Geller, E. K. Petrov, D. C. Raskazov, and G. A. Spiridonov, *Thermophysical Properties of FREONS, Methane Series, Part 1* (Hemisphere, Washington, DC, 1987).
11. C. I. Ivanchenko, Author's abstract of candidate thesis (OTIFI, Odessa, 1974).
12. D. C. Raskazov, U. M. Babikov, and N. Y. Filatov, *Tr. Mosk. Energ. Inst.* **129**:62 (1974).
13. D. C. Raskazov, U. M. Babikov, and N. Y. Filatov, *Gosstandart SSSR, GSSSD* **8**:142 (1975).
14. D. C. Raskazov, U. M. Babikov, and N. Y. Filatov, *Tr. Mosk. Energ. Inst.* **234**:90 (1975).
15. N. G. Sagaedakova, Author's abstract of candidate thesis [LT(Kh)P, Leningrad, 1977].
16. M. Takahashi, S. Takahashi, and H. Iwasaki, *J. Chem. Eng. Data* **30**:10 (1985).
17. M. Takahashi, C. Yokoyama, and S. Takahashi, *J. Chem. Eng. Data* **32**: 98 (1987).
18. M. Takahashi, C. Yokoyama, and S. Takahashi, *Int. Chem. Eng.* **27**:85 (1987).
19. M. Takahashi, C. Yokoyama, and S. Takahashi, *J. Chem. Eng. Data* **33**:267 (1988).
20. G. F. Newell, *J. Appl. Math. Phys.* **10**:160 (1959).
21. H. Iwasaki and J. Kestin, *Physica* **29**:1345 (1963).
22. K. Stephan, R. Krauss, and A. Laesecke, *J. Phys. Chem. Ref. Data* **16**:993 (1987).
23. R. T. Jacobsen and R. B. Stewart, *J. Phys. Chem. Ref. Data* **2**:757 (1973).
24. J. V. Sengers, in *Proceedings of the International School of Physics, Enrico Fermi, Course 51, Critical Phenomena*, M. S. Green, ed. (Academic Press, New York, 1971), p. 445.



25. J. V. Sengers, in *Transport Phenomena-1973*, J. Kestin ed. (AIP Conf. Proc. 11, 1973), p. 229.
26. R. S. Basu and J. V. Sengers, *J. Heat Trans. Trans. ASME* **101**:3 (1979); **101**:575 (1979).
27. R. S. Basu, J. V. Sengers, and J. T. R. Watson, *Int. J. Thermophys.* **1**:33 (1980).
28. R. Krauss, J. Luettmer-Strathmann, J. V. Sengers, and K. Stephan, *Int. J. Thermophys.* **14**:951 (1993).
29. T. Ohta, *Progr. Theor. Phys.* **54**: 1566 (1975).
30. T. Ohta and K. Kawasaki, *Progr. Theor. Phys.* **55**:1348 (1976).
31. J. C. Nieuwoudt and J. V. Sengers, *J. Chem. Phys.* **90**:763 (1990).
32. R. F. Berg and M. R. Moldover, *Phys. Rev.* **A42**:7183 (1990).
33. A. G. Aizpiri, A. Rey, J. Davila, R. G. Rubio, J. A. Zollweg, and W. B. Streett, *J. Phys. Chem.* **91**:3351 (1991)
34. K. Ohgaki, S. Umezono, and T. Katayama, *J. Supercrit. Fluid* **3**:78 (1990).
35. K. Hori, S. Okazaki, M. Uematsu, and K. Watanabe, *Proc. 8th Symp. Thermophys. Prop.*, J. V. Sengers, ed. (ASME, New York, 1982), p. 380.
36. G. A. Olchowy and J. V. Sengers, *Phys. Rev. Lett.* **61**:15 (1988).
37. J. Luettmer-Strathmann, J. V. Sengers, and G. A. Olchowy, *J. Chem. Phys.* **104**:3026 (1996).